J. Biomed. Eng. Res : 286-294, 2008

EEG Nonlinear Interdependence Measure of Brain Interactions under Zen Meditation

Hsuan-Yung Huang, Pei-Chen Lo

Department of Electrical and Control Engineering National Chiao Tung University, Taiwan, Republic of China
(Received April 14, 2008. Accepted July 30, 2008)

Abstract

This work investigates the characteristics of brain interactions of experienced Zen-Buddhist practitioners by obtaining multichannel EEG (electroencephalogram) data. Brain interactions were compared among three phases - 40-minute meditation (M), 5-minute Chakra-focusing practice (Z) and rest with closed eyes (R). The similarity index S, developed in nonlinear dynamical system theory, was employed to measure the degree of possibly asymmetric coupling. Meditators exhibited, overall, stronger interactions among multiple cortical areas in meditation stages M and Z than in the R state. This enhancement was greater in the M stage when the meditator was accompanied by a thought-free and fully consciousness state. In the high-frequency band (>13Hz), the interdependence was also higher in both meditation stages than at baseline rest. However, the interaction strength, especially in the posterior regions, was greatest in the Z stage, which involved internal attention. Few electrode pairs were observed with significant pair-wise asymmetry in the Z state. The similarity is a possible characteristic of dense reciprocal and strong mutual interactions between multiple cortical areas during meditation - especially in the Z state in the high-frequency band. These results demonstrate that profound Zen meditation induces various dynamic states in different phases of meditation, possibly reflected by nonlinear interdependence measure.

Key words : Zen Meditation; EEG (electroencephalogram); nonlinear dynamics; nonlinear interdependence

I. INTRODUCTION

As researchers outline the advantages of meditation, scientific exploration of meditation phenomena has been becomes significant [1]. Despite an active discussion of brain dynamics over recent years, interactions in the particular state of consciousness that is associated with Zen meditation have seldom been addressed. In Western society, most relevant works have reported upon scientific studies of such practices as Yoga, Transcendental Meditation (TM) [2, 3] and Japanese meditation [4, 5]. Zen meditation, originating more than 2,500 years ago, hadnot attracted attention until recently. This practice has been demonstrated to promote physiological and psychological health [6, 7]. Therefore, the characterization of the EEG activities in different meditation states may help to understand the neuronal network and CNS (central nervous system) properties of such states. One important goal is to assess the nature of the interaction between separate brain regions. A study of synchronous oscillations has been conducted to investigate the important mechanism by which specialized cortical and subcortical regions integrate their activity into different functions and on different spatial scales [8]. Measurement of brain interdependence becomes a matter of significance in understanding the meditation EEG. Although the predominant EEG findings have revealed an increase in alpha-theta range coherence during meditation [2- 4, 9-10], relatively little is known about the nonlinear synchronization of EEG during the meditation process.

Conventional EEG coherence involves possibly synchronous oscillations in different frequency bands. However, the characterization of the synchronization phenomenon is limited. For example, the coherence approach is insensitive to the direction of influence, and is corrupted by volume conduction and in nonlinear situations [11, 12]. A number of works have suggested that brain dynamics should be regarded as a large ensemble of coupled nonlinear dynamical subsystems. Accordingly, significant nonlinear synchronization has been detected on the macroscopic scales of EEG channels in healthy subjects [12-16]. Various types of synchronization based on nonlinear

Corresponding Author : Hsuan-Yung Huang
Department of Electricaland Control Engineering, National Chiao Tung University 1001 Ta-Hsueh Road, Hsinchu 30010, Taiwan, Republic of China
Tel : 886-3-571-2121 ext 54420 / Fax : 886-3-571-5998
Email : hsuany.ece88g@nctu.edu.tw, pclo@faculty.nctu.edu.tw
Running title: Brain Interdependence under Zen Meditation
EEG Nonlinear Interdependence Measure of Brain Interactions under Zen Meditation

dynamical theory have been demonstrated to be more effective in integrative neural processing [17] than narrow-band frequency synchronization as in the coherence function. Such "nonlinear coupling" allows the nonlinear interdependence among multi-recording sites to be examined and represents an alternative to the coherence function. Analyzing the reconstructed phase space yields information on such invariant quantities as phase synchronization [17], generalized synchronization [18] or synchronization likelihood [19], potentially revealing nonlinear structures that are hidden to standard linear methods [20, 21]. Theoretical studies have demonstrated that such indices cannot reveal any causal relationship among signals [22]. Besides, determining both the significance and the nonlinearity of interdependence depends on the use of additional statistical tests [23]. Several authors have thus proposed more robust sets of measures [22, 24, 25]. One method is called the *similarity index*, which, instead of estimating predictions, quantifies how neighborhoods (recurrences) in one attractor map into the other. This method has the advantages of sensitivity to nonlinear interdependence and the ability to detect asymmetric relationships that are hidden in the multi-electrode data [24, 26]. Based on the concept, the modified similarity index allows the implementation parameters to be better chosen and the degree of interactions to be effectively determined even under noisy conditions. The effectiveness of this method in characterizing the nonlinear interdependence behaviors of brain dynamics during Zen meditation was thus investigated.

Nonlinear interdependence measurement has been demonstrated to elucidate brain dynamics in various physiological, pathological or mental states. It has been applied to the analysis of normal resting adults subjects [12, 13], distinctive auditory processing of music by musicians and non-musicians [27, 28], and healthy-term neonates while awake or sleep [29]. This study focuses on the nonlinear dynamical behaviors of the brain during Zen meditation. Resent EEG findings of well experienced practitioners show an increase of dimensional complexity [30].This work thus further explores the nonlinear interdependence of multichannel scalp EEG from experienced Zen-meditation practitioners.

II. MATERIAL AND METHODS

A. Subjects and Procedures

In this study, 12 Zen-meditation practitioners (mean age: 32.5 year; range: 2841 years; 4 females; all right-handed) were examined. All subjects were long-term practitioners with an average of 8.8 years (range 5 to 13 years) of experience in Zen-Buddhist meditation practice. Normally, meditators participated in a 90 min group meditation session at least once a week and practiced 20-60 min of individual meditation daily. One important technique for good-quality Zen meditation is to guard and focus on a particular site (called a Chakra), such as the Zen Chakra inside the third ventricle (Introduction of Zen Meditation, by Master Wu Chueh Miao Tien, published by Zen Cosmos, 2004). By focusing on a Chakra, experienced practitioners reportedly can frequently enter into a tranquil state of consciousness that transcends the physiological (fifth), mental (sixth), subconscious (seventh) and Alaya (eighth) states of consciousness.

Within-subject behaviors throughout the meditation were examined. In the first three minutes, baseline EEG for each meditator under normal rest with closed eyes (R), non-meditative conditions was collected. The practitioners were then instructed to begin a 40 min meditation. After the meditation, the subjects were asked to keep their eyes closed for an additional 3 min transition period. They were then asked to practice Zen-Chakra focusing for 5 min. During the recording period, the subjects sat in the full-lotus position with eyes closed. Following the recording, the subjects were asked for an interview. Stage M refers to a 3 min artifact-free epoch soon after 30 min of meditation. Stage Z session refers to the first 3 min of artifact-free data segments during Zen-Chakra focusing.

B. EEG recordings

The EEG signals were recorded by the 30-channel, common -reference (linked-mastoid MS1-MS2) electrode montage based on the international 10-20 system. As the number of interdependence measure increases with the square of channel number, a data reduction was required. We thus selected the following 19 locations for analysis: Fp1, F7, F3, T7, C3, P7, P3, P1, Fz, Cz, Pz, Fp2, F8, F4, T8, C4, P8, P4, O2. EEG signals were sampled at 200 Hz after 0.3-45 Hz band-pass filtering. Each EEG epoch (R, M and Z) was analyzed by running measurement of nonlinear interdependence using a 5-second window without overlap.

C. Nonlinear interdependence measure

The algorithm for calculating nonlinear interdependence is described below. From time series simultaneously measured in two systems X and Y, we can reconstruct delay vectors $X_i = (x[i], x[i+\tau], \cdots, x[i+(m-1)\tau])$ and $Y_i = (y[i], y[i+\tau], \cdots, y[i+(m-1)\tau]), i = 1, \cdots, N$ where N is the total number of state points, m is the embedding dimension and τ denotes the delay in sample. A

KNN hypersphere, formed by the K's nearest neighboring (NN) points, is a cloud of K m-dimensional neighboring points around each X_i. Let $r_{i,j}$ and $s_{i,j}$, $j = 1, \cdots, K$, denote the time indices of the KNN points of X_i and Y_i, respectively. Then, K nearest neighbors of X_i are $X_{ri,j}$, $j = 1, \cdots, K$. For a given state point X_i, the mean-square Euclidean distance (or the average radius of the *cloud* centered at this state point) to its KNN is defined as:

$$R_i^{(K)}(X) = \frac{1}{K}\sum_{j=1}^{K} \| X_i - X_{ri,j} \|^2 \quad (1)$$

Another point cloud around X_i is formed with respect to its mutual neighbors $X_{si,j}$, which share the same temporal indexes of the KNN of Y_i. In this sense, the Y-conditioned mean-square Euclidean distance is defined by replacing the true nearest neighbors of X_i by the *mutual* neighbors [22]:

$$R_i^{(K)}(X|Y) = \frac{1}{K}\sum_{j=1}^{K} \| X_i - X_{si,j} \|^2 \quad (2)$$

The average square radius of X_i to all the remaining points in the phase space is given by

$$R_i(X) = \frac{1}{N-1}\sum_{j=1, j\neq i}^{N} \| X_i - X_j \|^2 \quad (3)$$

Then, for two strongly synchronized systems, both sets of neighbors, self and mutual, mostly coincide and $R_i^{(K)}(X) \approx R_i^{(K)}(X|Y) << R_i(X)$; whereas for independent systems, mutual neighbors are more scattered, which leads to $R_i^{(K)}(X) \approx R_i^{(K)}(X|Y) << R_i(X)$. Thus, the degree of interdependence of these two systems is reflected by the similarities (or dissimilarities) between these two cloud types formed by self and mutual neighbors, respectively. Accordingly, the strength of similarity between these two point clouds is termed as similarity index S [22, 24] and is defined below:

$$S^{(K)}(X|Y) = \frac{1}{N}\sum_{i=1}^{N} \frac{R_i^{(k)}(X)}{R_i^{(k)}(X|Y)} \quad (4)$$

$S^{(k)}(X|Y)$ works by directly assessing the statistical dependence of the state-space structure of X on that of Y in order to test whether closeness in X implies closeness in Y and *vice versa*. For identical systems (where the set of self nearest and mutual neighbors are identical) both these indexes equal to the maximum value (=1), whereas for completely independent systems, the indexes are close to zero. The opposite interdependence $(S^{(k)}(X|Y))$ can be computed analogically and they are in general asymmetric (i.e., $S^{(k)}(X|Y) \neq S^{(k)}(X|Y)$). $S^{(k)}(X|Y)$ assesses the effect of signal Y on signal X speaking in view of the system theory, signal Y is regarded as the source or the active role of activity. On the other hand, $S^{(k)}(X|Y)$ analysis considers Y as a sink or the passive role [22, 24]. The asymmetry of S is one of the main advantages over other nonlinear measures such as the mutual information and the phase synchronizations. The fact that S is asymmetric allows us to study not only topographic patterns but also functional properties. By considering each electrode either as a sink or as a source of activity, we may thereby get further information about the direction of the interaction [25].

In order to maximize the sensitivity to the underlying synchronizations and gain the robustness against noise, we proposed a modified version of S measure with adjusted range of KNN. Following our previous study of dimensional complexity index [30, 31], a reliable estimate of dimensional complexity of a system was obtained by averaging the complexity indexes over a moderate range of K's. A small K causes superimposed noise, while a large K results in a measurement involving multi-modal effects [30]. To determine a robust measure against noise, it follows that the final estimate of nonlinear interdependence is the averaged $S^{(k)}(X|Y)$ over an appropriate range of K's and is denoted by $S(X|Y)$.

There is no unique way to choose the implementing parameters. However, previous studies of dimensional complexity for meditation EEG have established a moderate choice of parameters as: $\tau = 5$, $m = 15$ and window length $N = 1000$ [30, 31]. The units of τ and N are samples. The time delay τ was determined by the first zero-crossing of the corresponding autocorrelation function. Embedding dimension m was determined by the convergent estimate. The final estimate, $S(X|Y)$, was obtained by averaging the $S^{(k)}(X|Y)$ computed with K ranging from 20 to 35.

D. Statistical analysis

Each set of 3-min EEG data was divided into 36 non-overlapping, consecutive 5sec segments. In each 5sec segment, S indices were calculated for 342 (=18×19) connective pairs of 19 electrodes. For each subject, data were averaged over 36 segments for each state. Means and standard deviations of

each state were then calculated. The Kolmogorov-Smirnov Goodness of Fit Test was adopted to justify the normal distribution of the results. Statistical differences between S indices were determined using paired Student's t-test to compare the baseline state R with the meditation states M and Z. Results that indicate significant difference (P<0.05) are presented below. For each pair of channels, the differences between the two stages were evaluated by calculating differences (d-value) between their mean S values, and then normalized to their standard deviation,

$$d = \frac{\overline{D}}{\sqrt{\frac{\sigma_D^2}{n}}}, D = S_Z - S_R \text{or } S_M - S_R \quad (5)$$

III. RESULTS

A. Interdependence matrix of meditating EEG

The results were expressed as a 19×19 interdependence matrix $S_{ij} = S(X_i|X_j)$. S_{ij} represents the coupling strength of the interaction of a given source, signal X_j, with respect to signal X_i. As displayed in Fig. 1, the result from a nine-year meditation practitioner during Z is encoded using an array of 19×19 colored boxes. The horizontal (vertical) electrode denotes $X_j(X_i)$. For instance, the lower-left box indicates the effect of conditioning O2 channel on channel Fp1. This figure is a typical example in showing stronger interdependence between the adjacent cortex and weaker interaction as the inter-electrode distance increases. The measured S is evidently asymmetric: the box (i,j) and its partner box (j,i) are generally unequal. Based on Fig. 1, the effect of occipital and posterior regions on anterior regions can be assumed to be weaker than the effect of anterior regions on the occipital and posterior regions.

For each subject, three S matrices were therefore derived from the R, M and Z states. A paired t-test was performed on each electrode pair S_{ij} to compare the different stages to understand the change in the overall topographic pattern with the stages. Lines with arrowheads indicate electrode pairs with significantly different synchronization (P<0.01) (Fig. 2). The strength of nonlinear synchronization (abbreviated to "NL-Syn") in the M state significantly exceeded that in the R state in one-third of electrode pairs (117 pairs, P<0.01). Most of

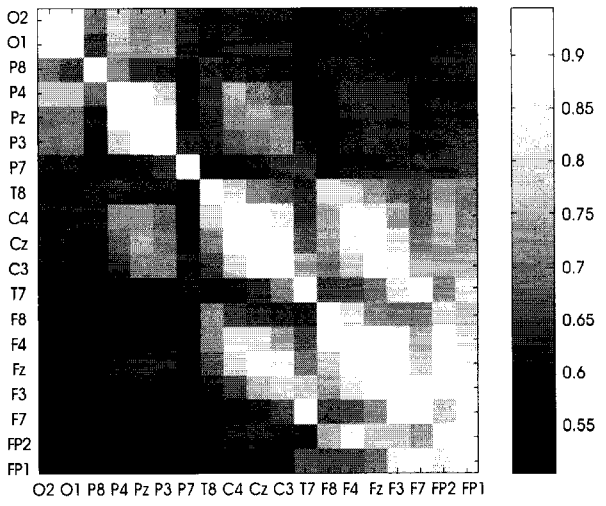

Fig. 1. Example for a 19×19 S-matrix of a 9-year meditator recorded during Z stage. For example, the leftmost bottom box represents S(Fp1|O2).

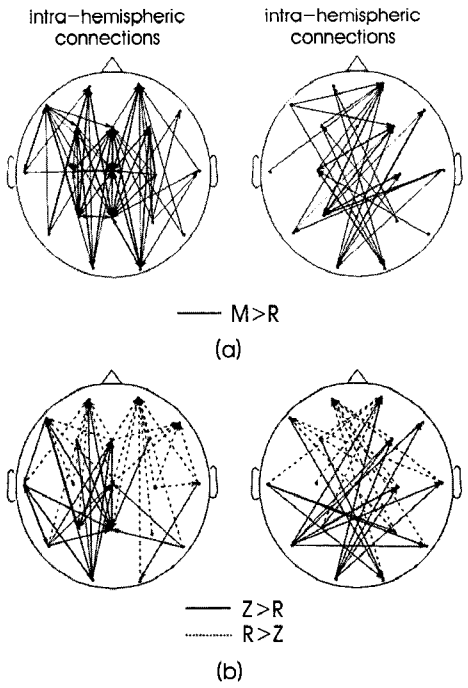

Fig. 2. A significant change of interdependence measure (P<0.01 or better) with respect to the baseline condition is mapped by arrowheaded lines between the electrode pair for the M state (a) and the Z state (b). The arrow represents a sink site.For better visual clarity, intra- and inter-hemispheric connections are displayed separately. Solid line indicates an increase and dashed line indicates a decrease of S measure.

the networks with increased S during the M stage, including both intra-and inter-hemispherical connections (Fig. 2 (a)), were formed between anterior and posterior electrodes. However, the S value in the Z state was significantly higher than in the R state in only 46 pairs (P<0.01). This increase was evident in the left anterior-to-posterior connections and the inter-hemispheric posterior connections (Fig. 2 (b)). However, the coupling of the other regions with the frontal electrodes in the Z state was significantly lower than in the R state (dashed lines in Fig 2 (b)). Overall, the meditators showed significantly higher synchronization over multiple cortical areas in meditation M or Z stages that in the resting state R. This enhancement was even greater in the M stage.

B. Asymmetry of meditation EEG

As mentioned in the preceding session, an important characteristic of the nonlinear interdependence measure S is its asymmetry. The differences between S (d-value) are displayed using a series of 19 brain maps to present the results of all 342 electrode-pair combinations. Each map shows the d values between the selected electrode (target) and the remaining 18 electrodes. The target acts a sink (source) on the maps of the left (right) column. The upper row of maps present the differences between the Z state and the baseline R state, while the lower maps plot the changes from the R state to the M state.

When each electrode was regarded as a source (right column, Fig. 3), the patterns of topographic changes differed. Firstly, significant differences between Z and R were evident at the temporal and occipital locations T7, P7 and O1 (P< 0.01, Z> R), whereas differences between M and R states were observed over the entire brain (P < 0.01, M>R), especially at the posterior electrodes, where the effect of the target site on the other electrodes was strongest.

The problem of pairwise asymmetry in these three stages was also studied. In both R and M states, significantly more pairs exhibited asymmetrical synchronization (P<0.01) than in the Z state: $S_{ij} \neq S_{ji}$ in 81 pairs in the R state and 79 pairs in the M state, while in the Z state, significant asymmetry (P<0.01) was evident in only 62 electrode pairs.

C. Measurement of nonlinear interdependence for high-frequency band

As stated elsewhere [30], EEG signals involve multi-rhythm patterns and dimensional complexity with multimodal dynamics. Additionally, the activity of the high-frequency band (>13Hz) increases significantly during deep meditation [30]. The detection of fast band synchronization, therefore, becomes critical to the understanding and characterization of brain function during meditation. Meditation EEGs were pre-filtered before interdependence analysis to elucidate the nonlinear interaction in the high-frequency band. This study considers EEG signals filtered through a sixth-order Butterworth band-pass filter with low and high cutoff frequencies of 13 and 45

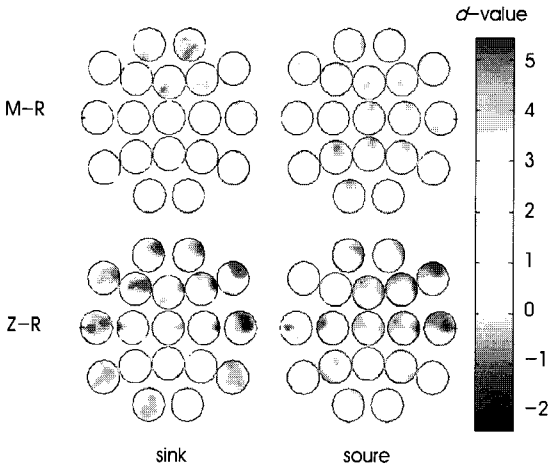

Fig. 3. Overall topographic differences of S (d-value) when the selected electrode was considered as a sink (left) and as a source (right) (d > 1.80, P < 0.05). The upper (bottom) row shows the differences between Z (M) state and R state.considered as a sink (left)

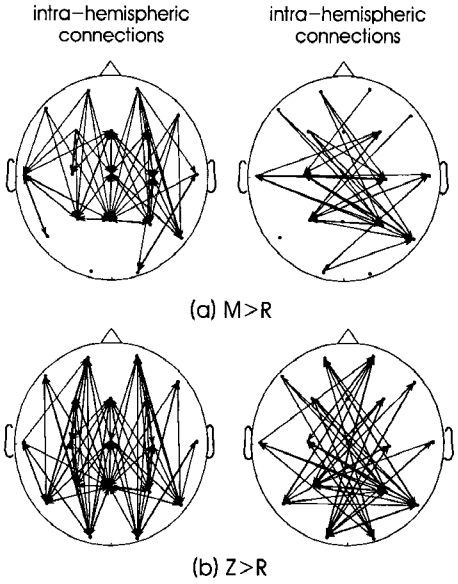

Fig. 4. The same expressions as Fig. 2 but for high-frequency band

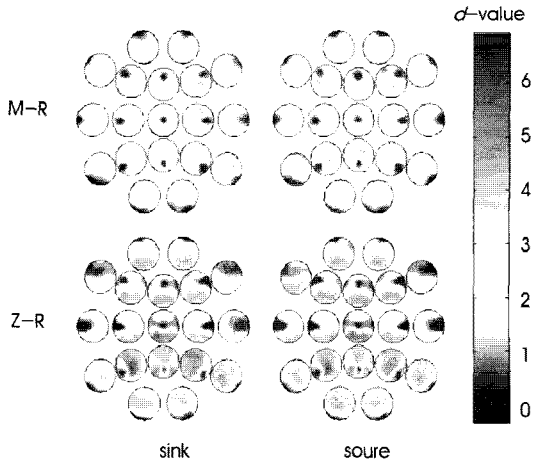

Fig. 5. The same expressions as Fig. 3 but for high-frequency band

Hz, respectively.

For each subject, the paired t-test was performed in each stage. Figure 4 plots the results. The electrode pairs associated with significantly different ($P<0.01$) synchronization are connected by arrowheaded lines. Apparently, the NL-Syn strength in the M state significantly exceeded the NL-Syn strength in the R state in approximately one-third of electrode pairs (115 pairs, $P<0.01$). The meditation-modulated networks reflected mainly the effects in the intra-hemispherical frontal and parietal regions (Fig. 4 (a)). The S values in the Z state markedly exceeded those in the R state, when the number of electrode pairs was higher (198 pairs, $P<0.01$). The increases were more accentuated for the intra- and inter-hemispheric connections from the anterior to the posterior electrodes (Fig. 4 (b)).

Figure 5, corresponding to Fig. 3, presents the brain maps of the d-value associated with high-frequency activity, when the target is treated as either a source (right column) or a sink (left column). Figures 3 and 5 differ in various ways. When target electrode is treated as a sink (left column, Fig. 5), the topographic differences between M and R stages are large at almost all electrodes. Noticeably, the differences between Zand R stages are even increased. A similar topographic change was observed when the target electrode was regarded as a source (right column, Fig. 5). The high-frequency band was associated with fewer asymmetrical interactions of electrode pairs ($S_{ij} \neq S_{ji}$). Significantly asymmetrical synchronization ($P<0.01$)was observed at only 42 (R state), 32 (M state) and 21 (Z state) pairs of electrode connections. Therefore, the fact that the degree of high-frequency synchronization was significantly higher when the Zen Chakra was guarded suggests that a strong network with dense reciprocal and symmetric interactions between cortical regions may have been formed in this state.

Ⅳ. DISCUSSION

This work is the first to describe the nonlinear-interdependence characteristics of brain interactions of experienced Zen meditators, based on multichannel EEG data that were recorded in the three phases R, M and Z. The S index revealed stage-related topographic differences in the interdependence of EEGs from various cortical regions. Meditators exhibited significantly enhanced interactions between multiple cortical areas in both meditation stages M and Z. Furthermore, the cause of the increased interdependence in stage M may be divided into the sinks in the right frontal regions and the sources in the central, occipito-parietal regions. The Z state was associated with different EEG oscillatory behaviors. The S value in the Z state exceeded that in the R state, but mainly in the left anterior-to-posterior connections and in the posterior regions. Diversely, the coupling strength in the direction from the other regions to the frontal electrodes was significantly lower in the Z state than in the R state.

Nonlinear interdependence in meditation EEG may produce stronger dynamical binding, with strong nonlinear coupling across a broad band of frequency. Moreover, the increased interdependence from the R state to the M state at the frontal regions is consistent with earlier studies. The previous EEG findings of most meditation studies have demonstrated increases in theta-alpha coherence, mostly in the frontal-central region [1-3]. Some of these studies have also claimed that high theta-alpha coherence is accompanied by thought- free, pure conscious experiences during meditation [10, 32]. In this work, eight of 12 meditators reported that they had experienced an M state with little thought but full consciousness. Such results may imply that enhanced coupling in the frontal region is related to low frequency band which is more

pronounced in the M state.

The degree of fast-band synchronization in both stages of meditation was significantly higher over all of the scalp electrodes. The increase was greater in the Z state (Fig. 4 (b)). It is likely due the specified meditation practice and mental strategy that affect the EEGs. Zen practitioners in this work were asked to focus on their Zen Chakra inside the third ventricle in the Z state this practice differed from other forms of meditation, which involve concentration on a mantra or on breathing. According to the post-experimental interviews, each meditator experienced a particular state of consciousness that involved mental quiescence with harmonic energy perception. These concentration techniques can be interpreted as methods of top-down control in which cortical processes are not determined by external stimuli but are driven by internal mental activity, mental imagery and other factors. Evidence showed that top-down processing may induce changes in gamma frequency activity or synchronization [33, 34]. Furthermore, neuronal oscillations and synchronization in the fast band play an important role in higher brain functions of consciousness [35, 36] and attentiveness [37, 38]. The enhancement in cortical synchrony in the gamma band has been proposed to be an integrative mechanism, which may bring a widely distributed set of neurons together into a coherent ensemble, underlying a conscious experience [39, 40]. Since the Z state involves internal attention that induces inner light, guarding the Zen Chakra may result in activation of attention-related networks and give rise to an internal percept in the visual cortex [41] that may also induce fast-band EEG synchronization. In such a situation, the enhancement of global, fast-band interdependence may indicate synchronization of massive distributive neural assemblies by the focusing process in the Z state.

With respect to asymmetrical properties, R and M states had significantly more pairs of asymmetrical synchronization than did the Z state. Moreover, balance of mutual influence became even more apparent for high frequency band in the two meditative states. Topographic differences between states showed similar patterns, despite the presence of a sink or source in the high-frequency band. These results suggest that the strengths of the effects of two cortical regions are comparable in both directions. Accordingly, this similarity possibly reflects stronger synchronization with dense reciprocal and mutual interactions between multiple cortical areas during meditation, especially in the Z state in the high frequency band. In summary, the overall interdependence patterns in the EEG of experienced Zen meditators during different phases were elucidated. This method makes it possible to determine that meditation is associated with different dynamics from baseline rest. Given the advantages of coupling asymmetry, measurements of S may provide more insights into the underlying mechanisms and be useful in investigating the cognitive processes in Zen meditation.

Figure 5, corresponding to Fig. 3, presents the brain maps of the d-value associated with high-frequency activity, when the target is treated as either a source (right column) or a sink (left column). Figures 3 and 5 differ in various ways. When target electrode is treated as a sink (left column, Fig. 5), the topographic differences between M and R stages are large at almost all electrodes. Noticeably, the differences between Z and R stages are even increased When the electrode is regarded as a sink (left column, Fig. 3), the topographic differences were large at posterior P3, P4 and Pz. That is, these electrodes tended to be influenced more by the remaining electrodes during Z (P<0.05). During M, this difference was even greater over almost of the whole brain, but especially in the frontal region (P< 0.001). Moreover, the interaction between multiple cortex regions was increased.

REFERENCES

[1] B. R. Cahn and J. Polich, "Meditation Statesand Traits: EEG, ERP, and Neuroimaging Studies." *Psychological Bulletin*, vol. 132,pp. 180-211, 2006.

[2] F. Travis and R.K. Wallace, "Autonomic and EEG patterns during eyes-closed rest and transcendental meditation (TM) practice: The basis for a neural model of TM practice," *Consciousness and Cognition*, vol. 8, pp.302-318, 1999

[3] F. Travis, J. Tecce, A. Arenander and R.K. Wallace, "Patterns of EEG coherence, power, and contingent negative variation characterize the integration of transcendental and waking states." *Biological Psychology*, vol. 61, pp. 293-319, 2002

[4] T. Murata; T. Takahashi; T. Hamada; M. Omori; H. Kosaka; H. Yoshida; Y. Wada, "Individual Trait Anxiety Levels Characterizing the Properties of Zen Meditation," *Neuropsychobiolog*, vol. 50, pp. 189-194, 2004

[5] M. Fumoto; I. Sato-Suzuki Y. Seki Y. Mohri H. Arita, "Appearance of high-frequency alpha band with disappearance of low-frequency alpha band in EEG is produced during voluntary abdominal breathing in an eyes-closed condition," *Neuroscience Research*, vol. 50, pp. 307-317, 2004

[6] P.C. Lo, M.L. Huang, K.M. Chang, "EEG Alpha blocking correlated with perception of inner light during Zen meditation." *Am. J. Chin. Med.*, vol. 31, pp.629-642, 2003

[7] K. M. Chang and P.C. Lo, "Meditation EEG Interpretation Based on Novel Fuzzy-Merging Strategies and Wavelet Features." *Journal of Biomedical Engineering-Applications, Basis & Communications*, vol. 17, pp.167-175, 2005

[8] W. Singer, "Consciousness and the binding problem," *Ann. NY. Acad. Sci.*, vol. 929, pp. 123-146, 2001

[9] M.C. Dillbeck and E.C. Bronson, "Short-term longitudinal

effects of the transcendental meditation technique on EEG power and coherence," *International Journal of Neuroscience*, vol. 14, pp. 147-151, 1981

[10] D.W. Orme-Johnson and C.T. Haynes, "EEG phase coherence, pure consciousness, creativity, and TM-Siddhi experiences," *International Journal of Neuroscience*, vol. 13, pp. 211-217, 1981

[11] P.L. Nunez, R.B.Silberstein, Z. Shi, M.R. Carpenter, R. Srinivasan, D.M. Tucker, S.M. Doran, P.J. Cadusch, and R.S. Wijesinghe, "EEG coherency. II. Experimental comparisons of multiple measures," *Clin Neurophysiol*, vol. 110, pp. 469-486, 1999

[12] M. Breakspear and J. R. Terry, "Detection and description of non-linear interdependence in normal multichannel human EEG data," *Clinical Neurophysiology*, vol 113, no. 5 , pp. 735-753, 2002.

[13] M. Breakspear and J. R. Terry, "Topographic organization of nonlinear interdependence in multichannel human EEG," *Neuroimage*, vol. 16, pp. 822-835, 2002

[14] C.J. Stam , T.C.A.M. van Woerkom, W.S. Pritchard, "Use of non-linear EEG measures to characterize EEG changes during mental activity," *Electroenceph Clin Neurophysiol*, vol. 99, pp.214-224, 1996.

[15] U. Feldmann, J. Bhattacharya, "Predictability improvement as an asymmetrical measure of interdependence in bivariate time series," *Int J Bifurcation Chaos*, vol. 14, pp. 505-514, 2004.

[16] C.J. Stam, M. Breakspear, A.M. van Cappellen van Walsum, and B.W. van Dijk, "Nonlinear Synchronization in EEG and Whole-Head MEG Recordings of Healthy Subjects," *Human Brain Mapping*, vol. 19, pp. 63-78, 2003.

[17] M.G. Rosenblum, A.S. Pikovsky and J. Kurths, "Phase synchronization of chaotic oscillators," *Phys. Rev. Lett.*, vol. 76, pp. 1804-1807, 1996

[19] C. J. Stam and B. W. van Dijk, "Synchronization likelihood: an unbiased measure of generalized synchronization in multivariate data sets," *Physica D* vol. 163, Issues 3-4, pp. 236-251, 2002

[18] S.J. Schiff, P. So, T. Chang, R.E. Burke and T. Sauer, "Detecting dynamical interdependence and generalized synchrony through mutual prediction in a neural ensemble," *Phys. Rev. E*, vol. 54, pp. 6708-6715, 1996

[20] E. Pereda, R. Quian Quiroga and J. Bhattacharya, "Nonlinear multivariate analysis of neurophysiological signals," *Progress in Neurobiology*, vol. 77, pp. 1-37, 2005

[21] C.J. Stam, "Nonlinear dynamical analysis of EEG and MEG: review of an emerging field," *Clin. Neurophysiol.* vol. 116, pp. 2266-2301, 2005

[22] R. Q. Quiroga, J. Arnhold, and P. Grassberger, "Learning driver-response relationships from synchronization patterns," *Phys. Rev. E*, vol. 61, no. 5, pp. 5149-5153, 2000.

[23] E. Pereda, R. Rial, A. Gamundi, and J. González, "Assessment of changing interdependencies between human electroencephalograms using nonlinear methods," *Physica D*, vol. 148, no. 12, pp. 147-158, 2001.

[24] J. Arnhold, P. Grassberger, K. Lehnertz and C. Elger , "A robust method for detecting interdependencies: application to intracranially recorded EEG." *Physica D* vol. 134, pp. 419-430, 1999.

[25] R. Quian Quiroga, A. Kraskov, T. Kreuz and P. Grassberger, "Performance of different synchronization measures in real data: a case study on electroencephalographic signals," *Phys. Rev. E*, vol. 65, pp. 041903-14, 2002.

[26] M. Le van Quyen, C. Adam, M. Baulac, J. Martenierie, and F. J. Varela, "Nonlinear interdependencies of EEG signals in human intracranially recorded temporal lobe seizures," *Brain Res.*, vol. 792, pp. 24-40, 1998.

[27] J. Bhattacharya, H. Petsche and E. Pereda, "Interdependencies in the spontaneous EEG while listening to music," *Int. J. Psychophysiol.* vol. 42, pp. 287-301, 2001

[28] J. Bhattacharya, E. Pereda and H. Petsche, "Effective detection of coupling in short and noisy bivariate data," *IEEE Trans. Syst. Man Cybern. B* vol. 33, pp. 85-95, 2003

[29] E. Pereda, S. Mañas, L. De Vera, J. M. Garrido, S. López, J. González, "Non-linear asymmetric interdependencies in the electroencephalogram of healthy term neonates during sleep," *Neuroscience Letters*, vol. 337, pp. 101-105, 2003.

[30] P.C. Lo and H.Y. Huang, "Investigation of Meditation Scenario by Quantifying the Complexity Index of EEG," *Journal of the Chinese Institute of Engineers*, vol. 30, no. 3, pp. 389-400, 2007.

[31] P.C. Lo and W.P. Chung, "An approach to quantifying the multi-channel EEG spatial-temporal feature," *Biometrical Journal*, vol. 42, pp. 21-34, 2000

[32] F. Travis, "Autonomic and EEG patterns distinguish transcending from other experiences during transcendental meditation practice." *International Journal of Psychophysiology*, vol. 42, pp. 19, 2001

[33] C. Tallon-Baudry, O. Bertrand, F. Peronnet and J. Pernier, "Induced gamma-band activity during the delay of a visual short-term memory task in humans," *J. Neurosci.* vol. 18, no. 11, pp. 4244-4254, 1998

[34] A. von Stein, C. Chiang and P. Konig, "Top-down processing mediated by interareal synchronization," Proc. Natl. Acad. Sci. USA 97 (2000) (26), pp. 14748-14753

[35] A. Lutz, J.-P. Lachaux, J. Martinerie and F.J. Varela, "Guiding the study of brain dynamics by using first-person data: synchrony patterns correlate with ongoing conscious states during a simple visual task," Proc. Natl. Acad. Sci. U. S. A. 99 (2002), pp. 1586-1591

[36] K.J. Meador, P.G. Ray, J.R. Echauz, D.W. Loring and G.J. Vachtsevanos, "Gamma coherence and conscious perception," *Neurology*, vol. 59, pp. 847-854, 2002

[37] M. Bauer, R. Oostenveld, M. Peeters and P. Fries, "Tactile spatial attention enhances gamma-band activity in somatosensory cortex and reduces low-frequency activity in parieto-occipital areas," *J. Neurosci.* vol. 26, pp. 490-501, 2006

[38] Ayelet N. Landau, Michael Esterman, Lynn C. Robertson, Shlomo Bentin, and William Prinzmetal, Different Effects of Voluntary and Involuntary Attention on EEG Activity in the Gamma Band, The Journal of Neuroscience, 31, 2007, 27(44) :11986-11990;

[39] C. Basar-Eroglu, D. Struber, M. Schurmann, M. Stadler and E. Basar, "Gamma-band responses in the brain: a short review of psychophysiological correlates and functional significance." *International Journal of Psychophysiology*, vol. 24, pp. 101-112, 1996

[40] O. Bertrand and C. Tallon-Baudry, "Oscillatory gamma activity in humans: a possible role for object representation." *International Journal of Psychophysiology*, vol. 38, pp. 211-223, 2000

[41] C. Tallon-Baudry, O. Bertrand, M.-A. Hénaff, J. Isnard and C. Fischer, "Attention Modulates Gamma-band Oscillations Differently in the Human Lateral Occipital Cortex and Fusiform Gyrus," *Cerebral Cortex*, vol. 15, pp. 654-662, 2005